Inorganic Chemistry
Article

trans-[Os^{III}(salen)(CN)$_2$]$^-$: A New Paramagnetic Building Block for the Construction of Molecule-Based Magnetic Materials

Jun-Fang Guo,[†] Wai-Fun Yeung,[†] Pui-Ha Lau,[†] Xiu-Teng Wang,[‡] Song Gao,*[,‡] Wing-Tak Wong,[§] Stephen Sin-Yin Chui,[§] Chi-Ming Che,*[,§] Wai-Yeung Wong,[∥] and Tai-Chu Lau*[,†]
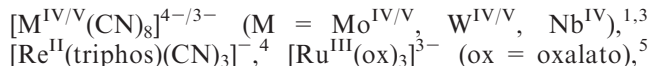
[†]*Department of Biology and Chemistry, City University of Hong Kong, Tat Chee Avenue, Kowloon Tong, Hong Kong, People's Republic of China,* [‡]*Beijing National Laboratory for Molecular Sciences, State Key Laboratory of Rare Earth Materials Chemistry and Applications, College of Chemistry and Molecular Engineering, Peking University, Beijing 100871, People's Republic of China,* [§]*Department of Chemistry, The University of Hong Kong, Pokfulam Road, Hong Kong, People's Republic of China, and* [∥]*Department of Chemistry, Hong Kong Baptist University, Waterloo Road, Hong Kong, People's Republic of China*

A novel dicyanoosmium(III) complex, *trans*-Ph$_4$P[Os^{III}(salen)(CN)$_2$]·CH$_2$Cl$_2$·H$_2$O (**1**; Ph$_4$P$^+$ = tetraphenylphosphonium cation, salen^{2-} = N,N'-ethylenebis(salicylideneaminato) dianion), has been synthesized and structurally characterized. Reactions of **1** with [Cu(Me$_3$tacn)(H$_2$O)$_2$](ClO$_4$)$_2$ (Me$_3$tacn = 1,4,7-trimethyl-1,4,7-triazacyclononane) under different conditions produce the 1-D ferromagnetic zigzag chains [Os(salen)(CN)$_2$]$_2$[Cu(Me$_3$tacn)]·CH$_3$OH (**2**) and [Os(salen)(CN)$_2$][Cu(Me$_3$tacn)]·ClO$_4$ (**3**).

Introduction

Paramagnetic 4d and 5d metal ions have been recognized recently as very appealing spin carriers for the preparation of molecular magnetic materials, since 4d and 5d orbitals are more diffuse than 3d orbitals and so enhanced magnetic interactions may be expected.[1] However, examples of polynuclear complexes based on 4d or 5d building blocks are rather limited. We note that 3d−4d and 3d−5d coordination polymers in the field of molecular magnetism are mostly constructed from precursors such as [Mo^{III}(CN)$_7$]$^{4-}$,[2]

[M$^{IV/V}$(CN)$_8$]$^{4-/3-}$ (M = Mo$^{IV/V}$, W$^{IV/V}$, Nb^{IV}),[1,3] [Re^{II}(triphos)(CN)$_3$]$^-$,[4] [Ru^{III}(ox)$_3$]$^{3-}$ (ox = oxalato),[5]

*To whom correspondence should be addressed. E-mail: bhtclau@cityu.edu.hk (T.-C.L.).

(1) Visinescu, D.; Desplanches, C.; Imaz, I.; Bahers, V.; Pradhan, R.; Villamena, F. A.; Guionneau, P.; Sutter, J.-P. *J. Am. Chem. Soc.* **2006**, *128*, 10202–10212.

(2) (a) Larionova, J.; Sanchiz, J.; Golhen, S.; Ouahab, L.; Kahn, O. *Chem. Commun.* **1998**, 953–954. (b) Sra, A. K.; Andruh, M.; Kahn, O.; Golhen, S.; Ouahab, L.; Yakhmi, J. V. *Angew. Chem., Int. Ed.* **1999**, *38*, 2606–2609. (c) Larionova, J.; Clérac, R.; Sanchiz, J.; Kahn, O.; Golhen, S.; Ouahab, L. *J. Am. Chem. Soc.* **1998**, *120*, 13088–13095. (d) Larionova, J.; Kahn, O.; Golhen, S.; Ouahab, L.; Clérac, R. *J. Am. Chem. Soc.* **1999**, *121*, 3349–3356. (e) Larionova, J.; Clérac, R.; Donnadieu, B.; Guérin, C. *Chem. Eur. J.* **2002**, *8*, 2712–2716. (f) Tanase, S.; Tuna, F.; Guionneau, P.; Maris, T.; Rombaut, G.; Mathonière, C.; Andruh, M.; Kahn, O.; Sutter, J.-P. *Inorg. Chem.* **2003**, *42*, 1625–1631. (g) Mironov, V. S.; Chibotaru, L. F.; Ceulemans, A. *J. Am. Chem. Soc.* **2003**, *125*, 9750–9760. (h) Le Goff, X. F.; Willemin, S.; Coulon, C.; Larionova, J.; Donnadieu, B.; Clérac, R. *Inorg. Chem.* **2004**, *43*, 4784–4786. (i) Chibotaru, L. F.; Hendrickx, M. F. A.; Clima, S.; Larionova, J.; Ceulemans, A. *J. Phys. Chem. A* **2005**, *109*, 7251–7257. (j) Milon, J.; Daniel, M.-C.; Kaiba, A.; Guionneau, P.; Brandes, S.; Sutter, J.-P. *J. Am. Chem. Soc.* **2007**, *129*, 13872–13878. (k) Gillon, B.; Goujon, A.; Willemin, S.; Larionova, J.; Desplanches, C.; Ruiz, E.; André, G.; Stride, J. A.; Guérin, C. *Inorg. Chem.* **2007**, *46*, 1090–1099.

(3) See, for example: (a) Chibotaru, L. F.; Mironov, V. S.; Ceulemans, A. *Angew. Chem., Int. Ed.* **2001**, *40*, 4429–4433. (b) Arimoto, Y.; Ohkoshi, S.-i.; Zhong, Z.-J.; Seino, H.; Mizobe, Y.; Hashimoto, K. *J. Am. Chem. Soc.* **2003**, *125*, 9240–9241. (c) Kashiwagi, T.; Ohkoshi, S.-i.; Seino, H.; Mizobe, Y.; Hashimoto, K. *J. Am. Chem. Soc.* **2004**, *126*, 5024–5025. (d) Song, Y.; Zhang, P.; Ren, X.-M.; Shen, X.-F.; Li, Y.-Z.; You, X.-Z. *J. Am. Chem. Soc.* **2005**, *127*, 3708–3709. (e) Sieklucka, B.; Podgajny, R.; Przychodzen, P.; Korzeniak, T. *Coord. Chem. Rev.* **2005**, *249*, 2203–2221. (f) Przychodzen, P.; Korzeniak, T.; Podgajny, R.; Sieklucka, B. *Coord. Chem. Rev.* **2006**, *250*, 2234–2260. (g) Visinescu, D.; Desplanches, C.; Imaz, I.; Bahers, V.; Pradhan, R.; Villamena, F. A.; Guionneau, P.; Sutter, J.-P. *J. Am. Chem. Soc.* **2006**, *128*, 10202–10212. (h) Atanasov, M.; Comba, P.; Lampeka, Y. D.; Linti, G.; Malcherek, T.; Miletich, R.; Prikhod'ko, A. I.; Pritzkow, H. *Chem. Eur. J.* **2006**, *12*, 737–748. (i) Lim, J. H.; Yoon, J. H.; Kim, H. C.; Hong, C. S. *Angew. Chem., Int. Ed.* **2006**, *45*, 7424–7426. (j) Prins, F.; Pasca, E.; Jos de Jongh, L.; Kooijman, H.; Spek, A. L.; Tanase, S. *Angew. Chem., Int. Ed.* **2007**, *46*, 6081–6084. (k) Wang, Z.-X.; Li, X.-L.; Liu, B.-L.; Tokoro, H.; Zhang, P.; Song, Y.; Ohkoshi, S.-i.; Hashimoto, K.; You, X.-Z. *Dalton Trans.* **2008**, *16*, 2103–2106. (l) Podgajny, R.; Pinkowicz, D.; Korzeniak, T.; Nitek, W.; Rams, M.; Sieklucka, B. *Inorg. Chem.* **2007**, *46*, 10416–10425. (m) Arai, M.; Kosaka, W.; Matsuda, T.; Ohkoshi, S.-i. *Angew. Chem., Int. Ed.* **2008**, *47*, 6885–6887. (n) Chelebaeva, E.; Larionova, J.; Guari, Y.; Ferreira, R. A. S.; Carlos, L. D.; Almeida, P.; Filipe, A.; Trifonov, A.; Guerin, C. *Inorg. Chem.* **2009**, *48*, 5983–5995.

(4) (a) Schelter, E. J.; Prosvirin, A. V.; Dunbar, K. R. *J. Am. Chem. Soc.* **2004**, *126*, 15004–15005. (b) Schelter, E. J.; Prosvirin, A. V.; Reiff, W. M.; Dunbar, K. R. *Angew. Chem., Int. Ed.* **2004**, *43*, 4912–4915. (c) Palii, A. V.; Ostrovsky, S. M.; Klokishner, S. I.; Tsukerblat, B. S.; Schelter, E. J.; Prosvirin, A. V.; Dunbar, K. R. *Inorg. Chim. Acta* **2007**, *360*, 3915–3924. (d) Schelter, E. J.; Karadas, F.; Avendano, C.; Prosvirin, A. V.; Wernsdorfer, W.; Dunbar, K. R. *J. Am. Chem. Soc.* **2007**, *129*, 8139–8149.

(5) Larionova, J.; Mombelli, B.; Sanchiz, J.; Kahn, O. *Inorg. Chem.* **1998**, *37*, 679–684.

$[Ru_2(O_2CR)_4]^+$,[6] $[Ru^{III}(acac)_2(CN)_2]^-$,[7] and $[Ru^{III}(salen)-(CN)_2]^-$,[7b,8] which exhibit various interesting magnetic properties.

Although there have been a number of reports on magnetic materials based on paramagnetic ruthenium centers, there are only two examples of magnetic materials containing paramagnetic osmium centers.[9] Dunbar reported the pentanuclear complex $\{[Ni(tmphen)_2]_3[Os(CN)_6]_2\}\cdot 6CH_3CN$ and the Prussian blue analogue $Ni_3[Os(CN)_6]_2\cdot 4H_2O$ constructed from $[Os(CN)_6]^{3-}$. Both compounds exhibit ferromagnetic coupling between Ni^{II} and Os^{III}.[9b] Herein we report the synthesis and characterization of a new paramagnetic dicyanoosmate(III) building block, trans-$[Os(salen)(CN)_2]^-$ (1; salen^{2-} = N,N'-ethylenebis(salicylideneaminato) dianion). Reactions of 1 with $[Cu(Me_3tacn)(H_2O)_2](ClO_4)_2$ (Me_3tacn = 1,4,7-trimethyl-1,4,7-triazacyclononane) under different conditions produce the 1-D ferromagnetic zigzag chains $[Os(salen)(CN)_2]_2[Cu(Me_3tacn)]\cdot CH_3OH$ (2) and $[Os(salen)-(CN)_2][Cu(Me_3tacn)]\cdot ClO_4$ (3).

Experimental Section

Materials and Reagents. All chemicals and solvents were of reagent grade and were used as received. $[Cu(Me_3tacn)-(H_2O)_2](ClO_4)_2$ was synthesized according to a literature method.[10] $Os^{II}(PPh_3)_3Cl_2$ was synthesized by an improved literature procedure.[11] $Os^{III}(salen)(PPh_3)Cl$ and 1 were synthesized by a method similar to that for $Bu_4N[Ru(salen)(CN)_2]$.[7b,12]

Instrumentation. IR spectra were recorded as KBr pellets on a Nicolet Avatar 360 FT-IR spectrophotometer at 4 cm^{-1} resolution. Elemental analyses were done on an Elementar Vario EL analyzer. Electrospray ionization mass spectra (ESI/MS) were obtained on a PE SCIEX API 365 mass spectrometer. Cyclic voltammetry was performed with a PAR Model 273 potentiostat using a glassy-carbon working electrode, a Ag/AgNO$_3$ (0.1 M in CH$_2$Cl$_2$) reference electrode, and a Pt-wire counter electrode with ferrocene (Cp$_2$Fe) as the internal standard. Magnetic measurements were performed on a Quantum Design MPMS XL-5 SQUID system. Background corrections were done by experimental measurements on the sample holder. The experimental susceptibilities were corrected for the diamagnetism of the constituent atoms (Pascal's tables).

Preparations. $Os^{II}(PPh_3)_3Cl_2$. A mixture of $(NH_4)_2[OsCl_6]$ (0.5 g, 1.14 mmol) and PPh$_3$ (2.1 g, 8.0 mmol) in 35 mL of a 5:2 2-methoxyethanol−water solvent mixture was refluxed for 3 h under argon. After the mixture was cooled to room temperature, the resulting green solid was collected by filtration, washed thoroughly with water and then methanol and diethyl ether, and dried in air. Yield: 1.1 g (92%).

$Os^{III}(salen)(PPh_3)Cl$. H$_2$salen (0.335 g, 1.25 mmol), triethylamine (0.5 g, 5 mmol), and $Os(PPh_3)_3Cl_2$ (1.05 g, 1.0 mmol) were refluxed in 50 mL of ethanol for 3 h. After it was cooled to room temperature, the solution was filtered and the filtrate was concentrated to about 5 mL. Addition of diethyl ether (50 mL) produced a dark brown precipitate which was collected by filtration and washed with water and then diethyl ether. Yield: 0.55 g (58%). Anal. Calcd for $C_{34}H_{29}N_2O_2PClOs$: C, 54.14; H, 3.88; N, 3.71. Found: C, 54.02; H, 4.21; N, 3.62.

trans-$Ph_4P[Os^{III}(salen)(CN)_2]\cdot CH_2Cl_2\cdot H_2O$ (1). $Os^{III}(salen)-(PPh_3)Cl$ (200 mg, 0.265 mmol) was refluxed with KCN (200 mg, 3.07 mmol) in 40 mL of ethanol for 4 h. The dark brown solution was evaporated to dryness and the residue then dissolved in 5 mL of water. Addition of Ph$_4$PCl (99 mg, 0.265 mmol) to the aqueous solution produced a dark brown precipitate which was collected, washed with water, and dried in vacuo. Well-defined dark brown block crystals were obtained by carefully layering diethyl ether over a CH$_2$Cl$_2$ solution of the product at room temperature for about 1 week. Yield: 72 mg (32%). Anal. Calcd for $C_{43}H_{38}$-$Cl_2N_4O_3OsP$: C, 54.32; H, 4.03; N, 5.89. Found: C, 54.35; H, 4.20; N, 5.92. IR (KBr): ν(C≡N) 2084(s) cm^{-1}. ESI/MS: m/z 510 $[Os^{III}(salen)(CN)_2]^-$.

$[Os(salen)(CN)_2]_2[Cu(Me_3tacn)]\cdot CH_3OH$ (2). $[Cu(Me_3tacn)-(H_2O)_2](ClO_4)_2$ (11 mg, 0.023 mmol) was dissolved in 2 mL of DMF in a test tube. 1 (20 mg, 0.023 mmol) dissolved in 8 mL of methanol was carefully layered above the DMF solution. Well-defined dark brown block crystals of 2 were obtained after leaving the test tube undisturbed at room temperature for about 1 week. Yield: 3 mg (21%). Anal. Calcd for $C_{46}H_{53}CuN_{11}O_5Os_2$: C, 43.03; H, 4.16; N, 12.00. Found: C, 42.86; H, 4.24; N, 11.93. IR (KBr): ν(C≡N) 2137, 2097 cm^{-1}.

$[Os(salen)(CN)_2][Cu(Me_3tacn)]\cdot ClO_4$ (3). Crystals of 3 were grown by slow interdiffusion in an H-shaped tube with 1 (33 mg, 0.038 mmol) in CH$_3$OH at one arm and $[Cu(Me_3tacn)-(H_2O)_2](ClO_4)_2$ (18 mg, 0.038 mmol) in DMF at the other. Brown microcrystals of 3 were formed on standing at room temperature after 3 days. Yield: 18 mg (57%). Anal. Calcd for $C_{27}H_{35}ClCuN_7O_6Os$: C, 38.48; H, 4.18; N, 11.63. Found: C, 38.11; H, 4.55; N, 11.60. IR (KBr): ν(C≡N) 2115 cm^{-1}.

Caution! Perchlorate salts of metal complexes with organic ligands are potentially explosive and should be handled in small quantities (< 50 mg) with care.

X-ray Crystallography. Measurements for compounds 1 and 2 were made on a Bruker SMART CCD diffractometer with graphite-monochromated Mo Kα radiation (λ = 0.710 73 Å). The structures were solved by direct methods (SHELXS97)[13] and expanded using Fourier techniques. All non-hydrogen atoms were refined anisotropically. All H atoms were refined using a riding model with $U_{iso}(H) = 1.2U_{eq}$(carrier).

X-ray Powder Diffraction. X-ray powder diffraction data of 3 were collected on a Bruker ADVANCE D8 diffractometer equipped with a motorized sample spinning stage. Intensity data were collected using the step-counting method (step size 0.02°), in continuous mode, in the 5 ≤ 2θ ≤ 70° range. Lattice parameters were determined by indexing the first 20 diffraction maxima within 5−20° (2θ) using the program DICVOL04.[14] The intensities of 132 Bragg diffraction peaks were extracted by

(6) (a) Cotton, F. A.; Kim, Y.; Ren, T. *Inorg. Chem.* **1992**, *31*, 2723–2726. (b) Beck, E. J.; Drysdale, K. D.; Thompson, L. K.; Li, L.; Murphy, C. A.; Aquino, M. A. S. *Inorg. Chim. Acta* **1998**, *279*, 121–125. (c) Liao, Y.; Shum, W. W.; Miller, J. S. *J. Am. Chem. Soc.* **2002**, *124*, 9336–9337. (d) Vos, T. Y.; Liao, Y.; Shum, W. W.; Her, J.-H.; Stephens, P. W.; Reiff, W. M.; Miller, J. S. *J. Am. Chem. Soc.* **2004**, *126*, 11630–11639. (e) Yoshioka, D.; Mikuriya, M.; Handa, M. *Chem. Lett.* **2002**, 1044–1045. (f) Vos, T. E.; Miller, J. S. *Angew. Chem., Int. Ed.* **2005**, *44*, 2416–2419. (g) Liu, W.; Nfor, E. N.; Li, Y.-Z.; Zuo, J.-L.; You, X.-Z. *Inorg. Chem. Commun.* **2006**, *9*, 923–925.

(7) (a) Yeung, W. F.; Man, W. L.; Wong, W. T.; Lau, T. C.; Gao, S. *Angew. Chem., Int. Ed.* **2001**, *40*, 3031–3033. (b) Yeung, W. F.; Lau, P. H.; Lau, T. C.; Wei, H. Y.; Sun, H. L.; Gao, S.; Chen, Z. D.; Wong, W. T. *Inorg. Chem.* **2005**, *44*, 6579–6590. (c) Yeung, W. F.; Lau, T. C.; Wang, X. Y.; Gao, S.; Szeto, L.; Wong, W. T. *Inorg. Chem.* **2006**, *45*, 6756–6760. (d) Toma, L. M.; Toma, L. D.; Delgado, F. S.; Ruiz-Pérez, C.; Sletten, J.; Canod, J.; Clemente-Juan, J. M.; Lloret, F.; Julve, M. *Coord. Chem. Rev.* **2006**, *250*, 2176–2193.

(8) (a) Duimstra, J. A.; Stern, C. L.; Meade, T. J. *Polyhedron* **2006**, *25*, 2705–2709. (b) Yoon, J. H.; Yoo, H. S.; Kim, H. C.; Yoon, S. W.; Suh, B. J.; Hong, C. S. *Inorg. Chem.* **2009**, *48*, 816–818.

(9) (a) Albores, P.; Slep, L. D.; Baraldo, L. M.; Baggio, R.; Garland, M. T.; Rentschler, E. *Inorg. Chem.* **2006**, *45*, 2361–2363. (b) Hilger, M. G.; Shatruk, M.; Prosvirin, A.; Dunbar, K. R. *Chem. Commun.* **2008**, 5752–5754.

(10) Fry, F. H.; Fischmann, A. J.; Belousoff, M. J.; Spiccia, L.; Brügger, J. *Inorg. Chem.* **2005**, *44*, 941–950.

(11) Hoffman, P. R.; Caulton, K. G. *J. Am. Chem. Soc.* **1975**, *97*, 4221–4228.

(12) Leung, W.-H.; Che, C.-M. *Inorg. Chem.* **1989**, *28*, 4619–4622.

(13) Sheldrick, G. M. *SHELX-97*; University of Gottingen, Göttingen, Germany, **1997**.

(14) Boultif, A.; Louer, D. *J. Appl. Crystallogr.* **2004**, *37*, 724–731.

Table 1. Summary of Crystallographic Data for **1** and **2**

	1	**2**
formula	$C_{43}H_{38}Cl_2N_4O_3OsP$	$C_{46}H_{53}CuN_{11}O_5Os_2$
formula mass (amu)	950.84	1283.93
cryst syst	triclinic	monoclinic
space group	$P\bar{1}$ (No. 2)	$P2_1/c$ (No. 14)
a (Å)	10.3519(6)	16.854(2)
b (Å)	12.8204(8)	13.4332(17)
c (Å)	15.8082(9)	21.843(3)
α (deg)	110.23(0)	90
β (deg)	93.36(0)	109.49(0)
γ (deg)	95.21(0)	90
V (Å^3)	1951.33(20)	4662.04(100)
Z	2	4
D_{calcd} (g cm^{-3})	1.618	1.829
T (K)	173(2)	296(2)
μ (mm^{-1})	3.491	5.948
$F(000)$	946	2508
no. of data/restraints/ params	8929/0/222	10 612/0/587
GOF on F^2	1.016	1.010
R1, wR2 ($I > 2\sigma(I)$)	0.030, 0.073	0.0576, 0.0255
R1, wR2 (all data)	0.032, 0.074	0.0404, 0.0638

a Pawley fit algorithm.[15] The structure solution was obtained by global optimization based on simulated annealing (SA) using the program DASH 3.1.[16] The input model for structure solution calculation was taken from the partial crystal structures of *trans*-[Os(salen)(SPh)$_2$][17] and [(pzTp)$_2$(Me$_3$tacn)$_3$Cu$_3$Fe$_2$(CN)$_6$]-(ClO$_4$)$_4$].[18] The input model was manually constructed by using the two fragments [Os(salen)(CN)] and [Cu(Me$_3$tacn)(CN)] using the molecular graphics suite program XP (SHELXTL version 6.14, Bruker AXS, 2000−2003). The structure of this chain structure was solved. Structural refinement on this model was performed using GSAS/EXPGUI software.[19]

Results and Discussion

Synthesis, Characterization, and Structures. Crystallographic data for compounds **1** and **2** are given in Table 1 and selected bond lengths and angles in Tables 2 and 3, respectively.

***trans*-Ph$_4$P[Os^{III}(salen)(CN)$_2$]·CH$_2$Cl$_2$·H$_2$O** (1). Compound **1** was prepared by the reaction of KCN with *trans*-[Os(salen)(PPh$_3$)Cl], similar to that for *trans*-Bu$_4$N-[Ru(salen)(CN)$_2$].[7b,12] The IR spectrum shows a strong $\nu(C\equiv N)$ stretch at 2084 cm^{-1}. The electrospray ionization mass spectrometry (ESI/MS) of a methanolic solution of **1** (Figure S1, Supporting Information) in the anionic mode shows a peak at m/z 510, which is due to the parent ion [Os(salen)(CN)$_2$]$^-$. There is an excellent agreement between the calculated and experimental isotopic distribution patterns.

The cyclic voltammogram of **1** in CH$_2$Cl$_2$ [0.1 M (Bu$_4$N)-PF$_6$] (Figure 1) shows two reversible waves at −0.15 and −1.47 V (vs Cp$_2$Fe$^{+/0}$), which are assigned to the Os^{IV}/Os^{III} and the Os^{III}/Os^{II} couples, respectively. These electrochemical data indicate that [Os(salen)(CN)$_2$]$^-$ is reasonably stable with respect to oxidation and reduction.

Table 2. Selected Bond Lengths (Å) and Angles (deg) for **1**

N1−Os1	2.004(3)	C17−Os1	2.081(4)
N2−Os1	1.996(3)	C18−Os1	2.070(4)
O1−Os1	2.032(3)	C17−N3	1.148(6)
O2−Os1	2.031(3)	C18−N4	1.150(6)
N2−Os1−N1	83.25(12)	O2−Os1−C18	89.18(11)
N2−Os1−O2	91.63(11)	O1−Os1−C18	91.61(11)
N1−Os1−O2	174.64(11)	N2−Os1−C17	93.59(12)
N2−Os1−O1	174.32(11)	N1−Os1−C17	87.15(12)
N1−Os1−O1	91.98(10)	O2−Os1−C17	91.63(11)
O2−Os1−O1	93.22(9)	O1−Os1−C17	89.23(11)
N2−Os1−C18	85.49(12)	C18−Os1−C17	178.79(14)
N1−Os1−C18	91.96(12)	N3−C17−Os1	176.85(33)
N4−C18−Os1	175.30(33)		

Table 3. Selected Bond Lengths (Å) and Angles (deg) for **2**^{a}

Os1−N6	1.998(3)	Os2−N7	2.002(4)
Os1−N5	2.003(4)	Os2−N8	2.006(4)
Os1−O2	2.023(3)	Os2−O3	2.030(3)
Os1−O1	2.035(3)	Os2−O4	2.042(4)
Os1−C1	2.048(4)	Os2−C4	2.066(5)
Os1−C2	2.060(4)	Os2−C3	2.068(5)
Cu1−N1	2.000(3)	Cu1−N10	2.208(4)
Cu1−N9	2.079(4)	Cu1−N11	2.210(4)
Cu1−N3	2.169(4)	Cu1−N2	2.224(4)
N1−C1^i	1.151(5)	N2−C2	1.155(6)
N3−C3	1.148(5)	N4−C4	1.146(6)
N6−Os1−N5	82.47(13)	N7−Os2−N8	82.90(16)
N6−Os1−O2	92.06(12)	N7−Os2−O3	92.10(14)
N5−Os1−O2	172.13(12)	N8−Os2−O3	174.89(14)
N6−Os1−O1	173.00(11)	N7−Os2−O4	175.01(14)
N5−Os1−O1	90.66(12)	N8−Os2−O4	92.13(14)
O2−Os1−O1	94.91(11)	O3−Os2−O4	92.87(11)
N6−Os1−C1	86.17(14)	N7−Os2−C4	87.73(16)
N5−Os1−C1	83.15(14)	N8−Os2−C4	90.91(18)
O2−Os1−C1	90.87(13)	O3−Os2−C4	90.00(17)
O1−Os1−C1	94.34(13)	O4−Os2−C4	91.91(15)
N6−Os1−C2	87.47(14)	N7−Os2−C3	92.13(16)
N5−Os1−C2	97.16(13)	N8−Os2−C3	88.76(16)
O2−Os1−C2	88.21(13)	O3−Os2−C3	90.33(15)
O1−Os1−C2	92.11(13)	O4−Os2−C3	88.20(15)
C1−Os1−C2	173.54(15)	C4−Os2−C3	179.65(19)
N1−Cu1−N9	172.81(14)	N3−Cu1−N11	173.84(14)
N1−Cu1−N3	91.00(14)	N10−Cu1−N11	81.32(13)
N9−Cu1−N3	91.18(14)	N1−Cu1−N2	92.02(12)
N1−Cu1−N10	90.99(14)	N9−Cu1−N2	94.71(13)
N9−Cu1−N10	81.97(14)	N3−Cu1−N2	92.92(13)
N3−Cu1−N10	95.88(14)	N10−Cu1−N2	170.65(13)
N1−Cu1−N11	94.52(14)	N11−Cu1−N2	89.63(13)
N9−Cu1−N11	83.01(14)	N1^{ii}−C1−Os1	166.84(33)
C1^i−N1−Cu1	157.17(29)	N2−C2−Os1	173.09(33)
C2−N2−Cu1	168.72(31)	N3−C3−Os2	175.94(41)
C3−N3−Cu1	166.29(37)	N4−C4−Os2	175.37(47)

^{a} Symmetry code: (i) $2 - x$, $1 - y$, $1 - z$.

Figure 1. Cyclic voltammogram of **1** in CH$_2$Cl$_2$.

(15) Pawley, G. S. *J. Appl. Crystallogr.* **1981**, *14*, 357–361.
(16) David, W. I.; Shankland, F. K.; van de Streek, J.; Pidcock, E.; Motherwell, W. D. S.; Cole, J. C. *J. Appl. Crystallogr.* **2006**, *39*, 910–915.
(17) Che, C. M.; Cheng, W. K.; Mak, T. C. W. *Inorg. Chem.* **1986**, *25*, 703–706.
(18) Gu, Z. G.; Liu, W.; Yang, Q. F.; Zhou, X. H.; Zuo, J. L.; You, X. Z. *Inorg. Chem.* **2007**, *46*, 3236–3244.
(19) (a) Larson, A. C.; Von Dreele, R. B. *Los Alamos National Laboratory Report LAUR 86-748*, **2004**. (b) Toby, B. H. *J. Appl. Crystallogr.* **2001**, *34*, 210–213.
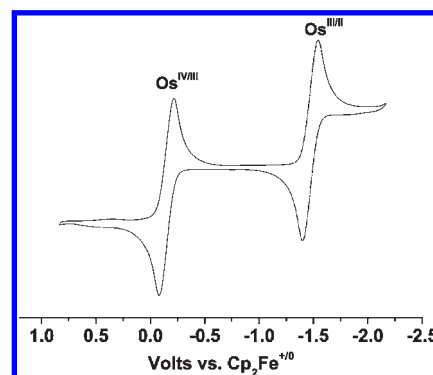
The X-ray structure of the anion of **1** is shown in Figure 2. The asymmetric unit consists of one [Os^{III}-(salen)(CN)$_2$]$^-$ anion, one Ph$_4$P$^+$, one CH$_2$Cl$_2$, and one H$_2$O molecule. The osmium(III) center has a distorted-octahedral geometry and is coordinated to the two oxygen and two nitrogen atoms of salen in a planar manner, and the two cyanide groups are trans. The average Os−O, Os−N, Os−C and C≡N bond lengths are 2.031(3), 2.000(3), 2.076(4), and 1.149(6) Å, respectively. The C18−Os1−C17 angle is close to linear (178.79(14)°).
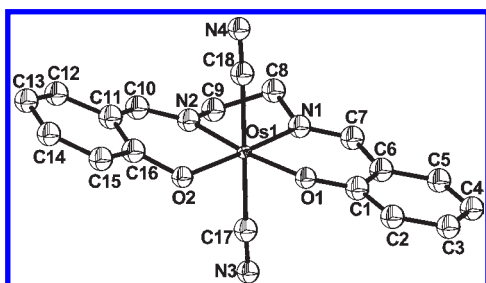
Figure 2. ORTEP view of [Os(salen)(CN)$_2$]$^-$ (the anion of **1**) with the atomic numbering scheme (30% probability).

The reaction of **1** with [Cu(Me$_3$tacn)(H$_2$O)$_2$](ClO$_4$)$_2$ in a CH$_3$OH/DMF solution using a layering technique produces **2** as dark brown block crystals. On the other hand, the same reaction carried out using an inter-diffusion technique in an H tube produces **3** as brown microcrystals. The IR spectrum of **1** shows a ν_{CN} stretch at 2084 cm^{-1}, whereas **2** shows two ν_{CN} stretches at 2137 and 2097 cm^{-1} and **3** shows a ν_{CN} stretch at 2115 cm^{-1}.

[Os(salen)(CN)$_2$]$_2$[Cu(Me$_3$tacn)]·CH$_3$OH (2). Compound **2** exists as a 1-D neutral zigzag polymer (Figure 3). The asymmetric unit consists of one [Cu-(Me$_3$tacn)]$^{2+}$ and two [Os(salen)(CN)$_2$]$^-$ ions. The [Os(salen)(CN)$_2$]$^-$ ions are in two different environments. One type of [Os(salen)(CN)$_2$]$^-$ is connected to two [Cu(Me$_3$tacn)]$^{2+}$ units using its trans cyano groups to form a zigzag chain with a N1−Cu1−N2 bond angle of 92.02(12)°. The other type of [Os(salen)(CN)$_2$]$^-$ ion is connected to [Cu(Me$_3$tacn)]$^{2+}$ using only one of its cyano groups. The Cu^{II} is hexacoordinated to six nitrogen atoms, three from the Me$_3$tacn ligand and three from bridging cyanide ligands, in a slightly distorted octahedral geometry. The average Cu−N(Me$_3$tacn) (2.166 Å) and Cu−N(cyano) bond lengths (2.131 Å) in
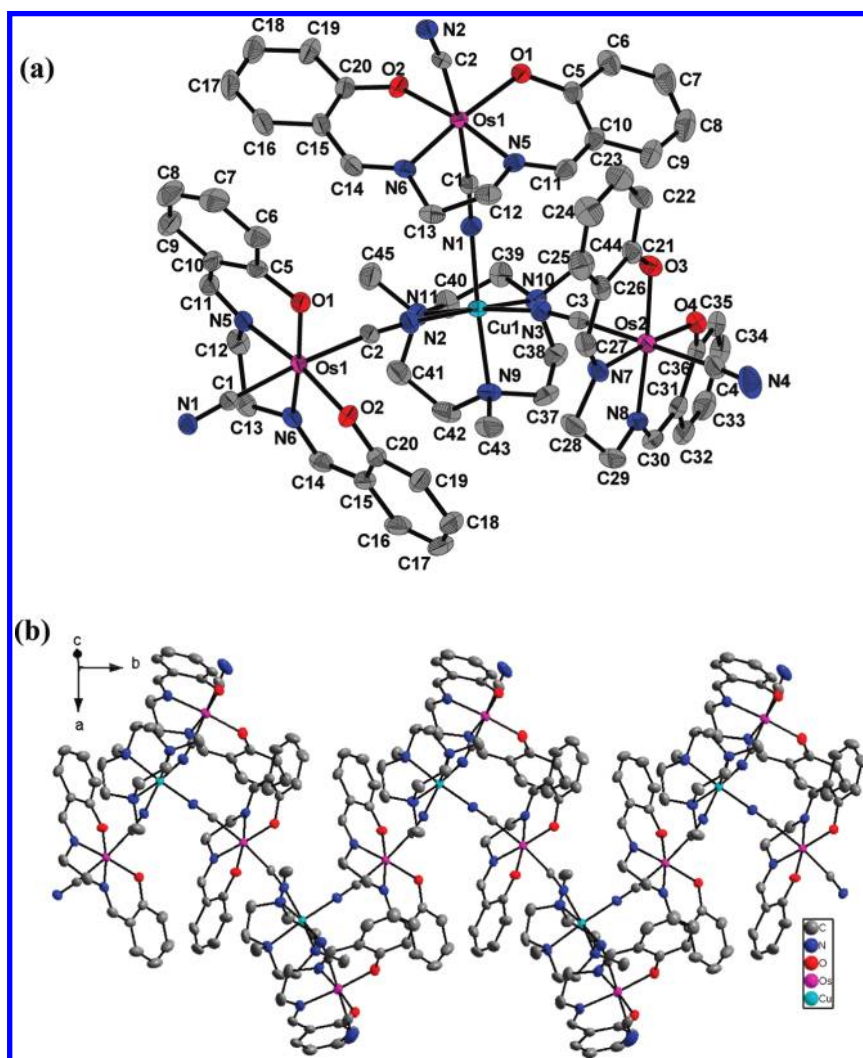
Figure 3. (a) ORTEP view of **2** with the atom-labeling scheme (30% probability). (b) Crystal-packing diagram of **2** projected down the *b* axis with the axes labeled. Hydrogen atoms and methanol molecules are omitted for clarity.

compound **2** are slightly longer than those in $[Tp_2(Me_3tacn)_3Cu_3Fe_2(CN)_6](ClO_4)_4 \cdot 2H_2O$ (Cu−N-(Me$_3$tacn) = 2.10 Å, Cu−N(cyano) = 1.98 Å).[20] The Cu−N≡C units are bent, with angles of 157.17(29), 166.29(37), and 168.72(31)° separately. The Os^{III} is also in a distorted-octahedral geometry: the salen ligand occupies the equatorial positions, and the two cyanide ligands are at the axial sites. The bond distances in each $[Os(salen)(CN)_2]^-$ unit (Os−O = 2.023(3)−2.042(4) Å; Os−N = 1.998(3)−2.006(4) Å; Os−C = 2.048(4)−2.068-(5) Å and C≡N = 1.146(6)−1.155(6) Å) are similar to those found in **1**. The Os−C≡N angles are bent with values of 166.84(33), 173.09(33), and 175.94(41)° for bridging and 175.37(47)° for terminal cyano groups. A classical hydrogen bonding interaction exists between the methanol solvate and one of the phenoxy oxygens (O1) of the salen ligand. The intramolecular Cu···Os distances are 5.3319(4) and 5.3880(5) Å. The shortest intrachain Os···Os and Cu···Cu separations are 7.09679(19) and 10.0583(6) Å, respectively, while the shortest interchain Os···Os and Cu···Cu distances are 8.0055(2) and 7.3402(3) Å, respectively.

$[Os(salen)(CN)_2][Cu(Me_3tacn)]\cdot ClO_4$ (3). Since the crystals of **3** were too small for single-crystal X-ray diffraction, the structure was solved by using X-ray powder diffraction data. The 1-D structure of **3** was confirmed by successful Rietveld refinement analysis of the powder diffraction data. The graphical plot of the final refinement cycle is shown in Figure 4a, and the results are given in Table 4. The structure of **3** is shown in Figure 4b, and selected bond lengths and bond angles are summarized in Table 5. Each $[Os(salen)(CN)_2]^-$ unit is connected to two $[Cu(Me_3tacn)]^{2+}$ units using its trans cyano groups to form a zigzag chain with a N4−Cu1−N3 bond angle of 79.08°. The perchlorate anions are situated between the polymeric chains. Each Cu^{II} center is penta-coordinated to five nitrogen atoms, three from Me$_3$tacn and two from cyano groups, in a distorted-square-pyr-amidal geometry. The average Cu−N(Me$_3$tacn) (2.095 Å) and Cu−N(cyano) bond lengths (2.107 Å) in compound **3** are slightly shorter than those in compound **2** (Cu−N(Me$_3$tacn) = 2.166 Å, Cu−N(cyano) = 2.131 Å). The Cu−N≡C units are virtually linear (178.62(14), 179.63(14)°). The Os^{III} is in a distorted-octahedral geo-metry: the salen ligand occupies the equatorial positions, and the two cyanide ligands are at the axial sites. The bond distances in each $[Os(salen)(CN)_2]^-$ unit (Os−O = 2.001(2)−2.007(3) Å; Os−N = 1.984(3)−2.000(2) Å; Os−C = 2.028(2)−2.045(2) Å) are comparable to those found in **2** and the monomeric complex **1**. One of the C≡N bond lengths is much shorter (1.015(2) Å) whereas the other one is slightly longer (1.188(3) Å) than those in **2** (1.146(6)−1.155(6) Å) and **1** (1.148(6)−1.150(6) Å). The Os−C≡N angles are almost linear (177.57(14) and 179.60(15)°). The intramolecular Cu···Os distances are 5.125 and 5.365 Å. The shortest intrachain Os···Os and Cu···Cu separations are 6.715 and 10.489 Å, respec-tively, while the shortest interchain Os···Os and Cu···Cu distances are 9.101 and 4.681 Å, respectively (Figure 4c).

Magnetic Properties.   Compound 1. The molar mag-netic susceptibility data of compound **1** indicate an unusually strong temperature-independent Van Vleck paramagnetism (temperature-independent paramagne-sitm, TIP) of 2.55×10^{-3} cm^3 mol^{-1}. After this TIP value was subtracted, the molar magnetic susceptibility in the temperature range 30−300 K of **1** obey the Curie−Weiss law ($\chi_M = C/(T - \Theta)$], with C = 0.45 cm^3 mol^{-1} K and Θ = −0.55 K (Figure 5). The C value is comparable to that of *trans*-Bu$_4$N[Ru(salen)(CN)$_2$] (0.414 cm^3 mol^{-1} K) and is near that of the low-spin (t$_{2g}$)^5 configuration with $S = ^1/_2$.[7b] The field dependence magnetization of **1** at 2.0 K is shown in the inset to Figure 5; the M value at 50 kOe is 1.02 $N\beta$ mol^{-1}, consistent with the expected saturation value for a $S = ^1/_2$ state with g = 2.0.

Compound 2. The temperature dependence of the mag-netic susceptibility of **2** was measured in the range of 2−300 K under an external magnetic field of 3 kOe (Figure 6). The molar magnetic susceptibility data of **2** also indicate an unusually strong temperature-independent Van Vleck paramagnetism (TIP) of 2.87×10^{-3} cm^3 mol^{-1}. The $\chi_M T$ value at room temperature is 1.36 cm^3 mol^{-1} K, which is larger than the spin-only value of 1.125 cm^3 mol^{-1} K for one Cu^{II} with $S = ^1/_2$ and two Os^{III} centers with $S = ^1/_2$. When the temperature is lowered, the $\chi_M T$ value increases smoothly and attains a maximum value of 1.94 cm^3 mol^{-1} K at 5 K; it then decreases sharply and reaches a value of 1.78 cm^3 mol^{-1} K at 2.0 K. After the TIP value is subtracted, the molar magnetic susceptibility above 30 K obeys the Curie−Weiss law, $\chi_M = C/(T - \Theta)$, with a Curie constant C = 1.33 cm^3 mol^{-1} K and a Weiss constant Θ = +3.96 K. The positive Θ value and the increasing $\chi_M T$ above 5 K indicate typical ferromagnetic coupling between Os^{III} and Cu^{II} in **2** through a cyano bridge. The abrupt decrease at low temperature may be due to the antiferro-magnetic interactions between CuOs chains and/or the field saturation effect. The magnetization of this compound per $[CuOs_2]$ unit reaches a value of 2.62 $N\beta$ mol^{-1} at 2.0 K and 50 kOe external field (Figure 5 inset), which is slightly lower than the expected saturation value of 3.0 $N\beta$ for the sum of two Os^{III} and one Cu^{II} magnetic moments ($S_T = 2S_{Os} + S_{Cu} = ^3/_2$; $M_S = gS_T N\beta$). The field-dependence magnetization has also been analyzed using Brillouin functions with $S = ^1/_2$. The experimental $M - H$ curve is above the Brillouin function curve below 24 kOe, which suggests ferromagnetic coupling between Os^{III} and Cu^{II} ions.

To evaluate the value of the exchange constants of **2**, we used an approximate approach similar to that for 1-D, 2-D, and quasi-2D complexes.[21] Cyanide bridges between Cu^{II} and Os^{III} were regarded equal, since the bridging modes through C1N1, C2N2, and C3N3 were almost the same. Therefore, the 1-D chain can be treated as the repeating unit of Os$_2$Cu trimers with the same intratrimer and intertrimer exchange constant J. For a Cu^{II}Os$^{III}_2$ trinuclear compound with $S_{Cu} = ^1/_2$ and $S_{Os} = ^1/_2$, we regard the **g** tensors as equal. The spin Hamiltonian is

$$H = -2J(S_{Cu}S_{Os1} + S_{Cu}S_{Os2})$$

(20) Wang, C. F.; Zuo, J. L.; Bartlett, B. M.; Song, Y.; Long, J. R.; You, X. Z. *J. Am. Chem. Soc.* **2006**, *128*, 7162–7163.

(21) (a) Kou, H. -Z.; Zhou, B. C.; Gao, S.; Liao, D.-Z.; Wang, R.-J. *Inorg. Chem.* **2003**, *42*, 5604–5611. (b) Chiari, B.; Cinti, A.; Piovesana, O.; Zanazzi, P. F. *Inorg. Chem.* **1995**, *34*, 2652–2657. (c) Caneschi, A.; Gatteschi, D.; Melandri, M. C.; Rey, P.; Sessoli, R. *Inorg. Chem.* **1990**, *29*, 4228–4234.
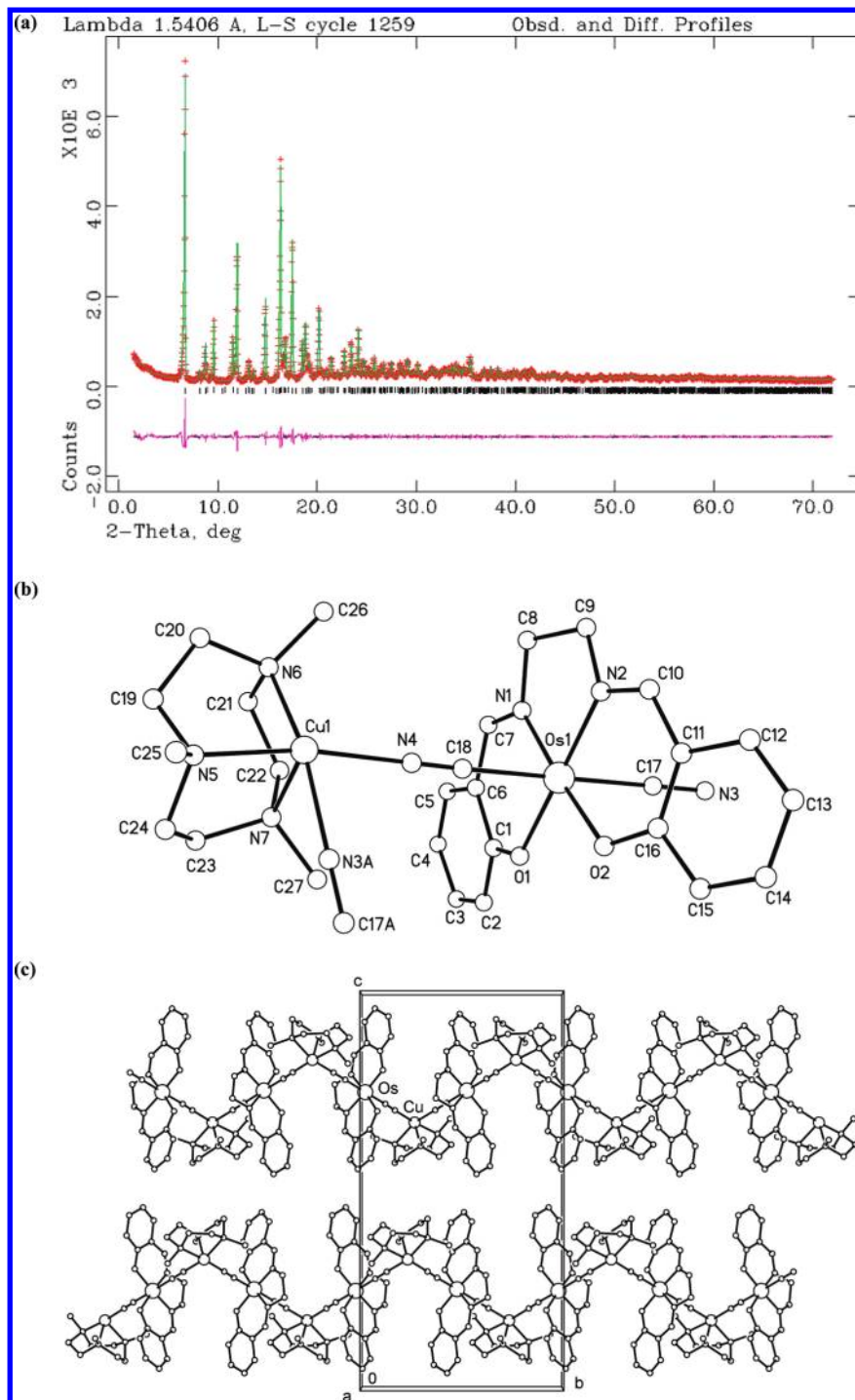
Figure 4. (a) Graphical plot of the final refinement cycle of **3**: observed (red line), calculated (green line), and difference X-ray diffraction data (magenta line) and Bragg peak positions (black ticks)]. (b) Ball and stick diagram of the building unit of **3** with the atom-labeling scheme. (c) View of the 1-D zigzag chains of **3**. All hydrogen atoms and the anion ClO_4^- are omitted for clarity.

Thus, the molar magnetic susceptibility of the triangular trimer[22] can be expressed as

$$\chi_t = \frac{Ng^2\beta^2}{4kT}\frac{1 + \exp(2J/kT) + 10\exp(3J/kT)}{1 + \exp(2J/kT) + 2\exp(3J/kT)}$$

Also, the molar magnetic susceptibility of the trimer

is written as

$$\chi_t = \frac{Ng^2\beta^2}{3kT}S_t(S_t + 1)$$

Then, the magnetic susceptibility of the chain is.

$$\chi_c = \frac{Ng^2\beta^2}{3kT}\frac{1+u}{1-u}S_t(S_t + 1)$$

Here $u = \coth(JS_t(S_t + 1)/kT - kT/JS_t(S_t + 1))$.

(22) Kahn, O. *Molecular Magnetism*; VCH: New York, 1993.

Table 4. Results of the Structural Refinement of **3** using Powder X-ray Diffraction Data

formula	$C_{27}H_{35}ClCuN_7O_6Os$
formula mass (amu)	842.82
cryst syst	monoclinic
space group	$C2/c$ (No. 15)
a (Å)	26.3735(8)
b (Å)	13.4268(4)
c (Å)	18.3958(6)
α (deg)	90
β (deg)	92.237(3)
γ (deg)	90
V (Å^3)	6509.2(3)
λ (Å)	1.5406
Z	8
D_{calcd} (g cm^{-3})	1.720
no. of rflns, N	1522
no. of restraints, R	248
no. of variables, P	280
max (mean) (shift/esd^2)	0.10 (0.01)
wR_p, $R_p{}^a$	0.081, 0.060
R_{F^2}, χ^a	0.087, 1.39

^{a} $R_P = \sum |y_{i,o} - y_{i,c}|/\sum |y_{i,o}|$, $wR_P = [\sum w_i(y_{i,o} - y_{i,c})^2/\sum w_i y_{i,o}{}^2]^{1/2}$, and $R_{F^2} = \sum |F^2_{k,o} - F^2_{k,c}|/\sum F^2_{k,o}$, where y_i and F^2_k are the (observed and calculated) profile intensities and squared structure factors, respectively, w_i is a statistical weighting factor, taken as $1/y_{i,o}$, and i runs over all data points and k over the space group permitted reflections, and $\chi = [\sum w_i(y_{i,o} - y_{i,c})^2/(N - P)]^{1/2}$, where P is the number of refined variables and N the number of extracted and integrated reflections.

**Table 5.** Selected Bond Lengths (Å) and Angles (deg) for **3**^{a}

Cu1−N4	2.083(2)	Os1−C18	2.028(2)
Cu1−N7	2.050(3)	Os1−O2	2.001(2)
Cu1−N6	2.191(2)	Os1−O1	2.007(3)
Cu1−N5	2.043(2)	Os1−N2	1.984(3)
Cu1−N3	2.132(2)	Os1−N1	2.000(2)
N4−C18	1.015(2)	Os1−C17	2.045(2)
N3−C17	1.188(3)		
N4−Cu1−N7	90.43(5)	O2−Os1−C18	97.34(7)
N4−Cu1−N5	170.64(6)	O1−Os1−C18	86.40(7)
N5−Cu1−N7	85.13(5)	N2−Os1−C18	95.48(6)
N4−Cu1−N3	79.08(5)	N1−Os1−C18	84.09(6)
O1−Os1−N2	175.41(7)	C17−Os1−C18	178.88(7)
O1−Os1−N1	93.86(6)	O1−Os1−O2	89.70(6)
O1−Os1−C17	94.41(7)	O2−Os1−N2	94.20(6)
N1−Os1−N2	82.20(5)	O2−Os1−N1	176.25(6)
N2−Os1−C17	83.76(6)	O2−Os1−C17	81.91(6)
N1−Os1−C17	96.61(6)	Cu1−N4−C18	178.62(14)
N4−C18−Os1	177.57(14)	Cu1−N3(i)−C17(i)	179.63(14)
Os1−C17−N3	179.60(15)		

^{a} Symmetry codes: (i) $1.5 - x$, $-0.5 + y$, $-0.5 - z$.

On the basis of the molecular field theory, the molar susceptibility of compound **2** can be modified to include the interchain coupling as

$$\chi_M = \frac{\chi_c}{1 - (2zJ'/Ng^2\beta^2)\chi_c}$$

where J' is the interchain exchange coupling constant and z is the number of the nearest neighbor chains. The best fitting in the temperature range of 3−300 K gives $J = +1.56$ cm^{-1}, $zJ' = -0.76$ cm^{-1} and $g = 2.19$ with $R = 2.59 \times 10^{-4}$ ($R = \sum[(\chi_M T)_{obsd} - (\chi_M T)_{calcd}]^2/\sum(\chi_M T)_{obsd}{}^2$). The positive value of exchange coupling through the cyanide bridges suggests ferromagnetic interaction between Cu^{II} and Os^{III} centers, and the relatively large negative value of zJ' indicates antiferromagnetic interaction between the neighboring Cu^{II}Os^{III} chains,
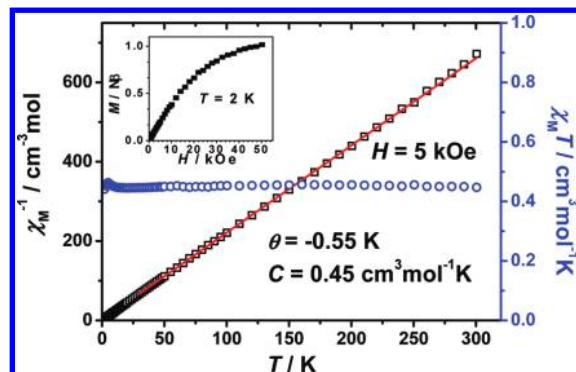
Figure 5. Temperature dependence of $\chi_M T$ (circles) and $\chi_M{}^{-1}$ (squares) for **1**.
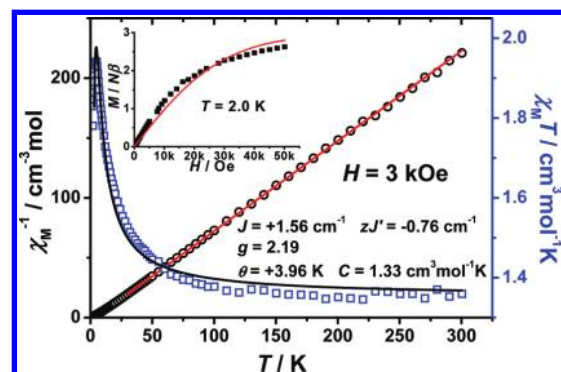
Figure 6. Temperature dependence of $\chi_M T$ (squares) and $\chi_M{}^{-1}$ (circles) for **2**. The inset shows the field dependence of the magnetization (squares) and the Brillouin function curve (line).
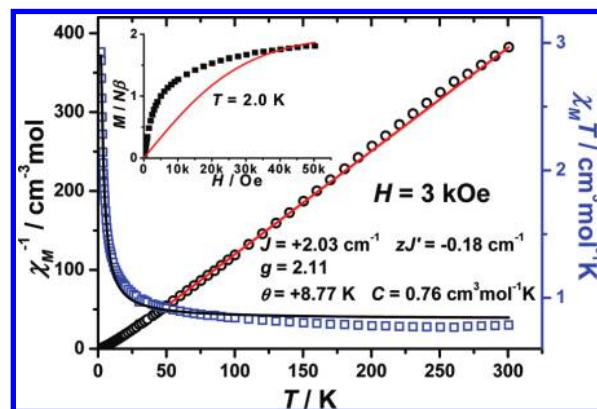
Figure 7. Temperature dependence of $\chi_M T$ (squares) and $\chi_M{}^{-1}$ (circles) for **3**. The inset shows the field dependence of the magnetization (squares) and the Brillouin function curve (line).

which results in the sharp decrease of $\chi_M T$ value below 5 K. The ZFC-FC plot (Figure S2, Supporting Information) indicates that no long-range ordering occurs above 2 K.

Compound 3. The magnetic properties of **3** were measured under an external field of 3 kOe in the range of 2−300 K (Figure 7). The $\chi_M T$ value at room temperature is 0.786 cm^3 mol^{-1} K, which is close to the spin-only value of 0.75 cm^3 mol^{-1} K for one Cu^{II} ($S = 1/2$) and one Os^{III} ($S = 1/2$). When the temperature is lowered, the $\chi_M T$ value increases smoothly and attains a maximum value of 2.93 cm^3 mol^{-1} K at 2 K. Fitting the data above 50 K

with the Curie–Weiss law ($\chi_M = C/(T - \Theta)$] gives $C = 0.76$ $cm^3\,mol^{-1}$ K and $\Theta = +8.77$ K. The positive Θ value indicates a ferromagnetic interaction between Os^{III} and Cu^{II} through the cyanide bridge, which is expected from the orthogonality of the magnetic orbitals of the metal ions. The magnetization of this compound per [CuOs] unit reaches a value of 1.81 $N\beta$ mol^{-1} at 2.0 K and 50 kOe (Figure 7 inset), nearly consistent with the expected saturation value of 2.0 $N\beta$ for the sum of one Os^{III} and one Cu^{II} magnetic moment. The experimental $M - H$ curve of **3** is above the Brillouin function curve below 40 kOe, which suggests ferromagnetic coupling between Os^{III} and Cu^{II} ions. Using an approximate approach similar to that for compound **2**, the 1-D chain of **3** can be treated as the repeating unit of CuOs dimers with the same intradimer and interdimer exchange constant J; the magnetic susceptibilities can be expressed by the following equation[22] derived from the isotropic exchange spin Hamiltonian $H = -2JS_AS_B$:

$$\chi_d = \frac{2Ng^2\beta^2}{kT}\frac{1}{3+\exp(-2J/kT)} = \frac{Ng^2\beta^2}{3kT}S_d(S_d+1)$$

$$\chi_c = \frac{Ng^2\beta^2}{3kT}\frac{1+u}{1-u}S_d(S_d+1)$$

Here $u = \coth(JS_d(S_d+1)/kT - kT/JS_d(S_d+1)$.

$$\chi_M = \frac{\chi_c}{1-(2zJ'/Ng^2\beta^2)\chi_c}$$

The susceptibilities from 2 to 300 K were simulated, giving the best fit with the parameters $J = +2.03$ cm^{-1}, $zJ' = -0.18$ cm^{-1}, and $g = 2.11$ with $R = 1.49 \times 10^{-3}$ ($R = \sum[(\chi_MT)_{obsd} - (\chi_MT)_{calcd}]^2/\sum(\chi_MT)_{obsd}^2$). These results indicate a ferromagnetic interaction between Cu^{II} and Os^{III} centers. The ZFC-FC plot (Figure S3, Supporting Information) indicates that no long-range ordering occurs above 2 K.

Concluding Remarks

Two 1-D zigzag $Cu^{II}Os^{III}$ chains based on a new paramagnetic osmium(III) building block, *trans*-[Os(salen)(CN)$_2$]$^-$, have been synthesized and structurally characterized. They all exhibit intrachain ferromagnetic coupling between Cu^{II} and Os^{III} through cyanide ligands. The present work shows that [Os(salen)(CN)$_2$]$^-$ is a good building block for the construction of low-dimensional 3d–5d magnetic materials. The exchange interaction between Os^{III} and Cu^{II} in these two compounds is weak, which may be partially due to the Cu(II) ions having only $S = 1/2$. It is expected that the magnetic coupling would be stronger if the Cu^{II} ions were replaced by metal ions with larger spins (e.g., high-spin Mn^{III} or Fe^{III}), owing to greater radial extension of the d orbitals and higher degree of electron density delocalization over the bridging cyanides. The synthesis of various $Mn^{III}Os^{III}$ polymers based on [Os(salen)(CN)$_2$]$^-$ is in progress.